atmosphere

Article

Formation Mechanisms of the "5·31" Record-Breaking Extreme Heavy Rainfall Process in South China in 2021

Fangli Chen [1], Huiqi Li [2,3], Sheng Hu [2,3,*], Shuai Jiang [1,4], Jiaojiao Li [1,4] and Ruoting Wu [1]

1 Huizhou Meteorological Bureau, Huizhou 516001, China
2 Guangzhou Institute of Tropical and Marine Meteorology, China Meteorological Administration, Guangzhou 510641, China
3 China Meteorological Administration Tornado Key Laboratory, Guangzhou 510641, China
4 Huizhou Emergency Early Warning Information Release Center of Guangdong Province, Huizhou 516001, China
* Correspondence: sheng_hu@gd121.cn

Abstract: Based on the fifth-generation European Center for Medium-Range Weather Forecasts reanalysis data (ERA5), the real-time observation data from weather stations, and the radar products in Guangdong Province, we analyze the precipitation properties and formation mechanisms of the "5·31" extreme heavy rainfall process with record-breaking 3-h accumulated rainfall in South China during 2021. The results show that the extreme heavy rainfall process is caused by the joint actions of weather systems such as a weak upper-level short-wave trough, a surface stationary front, and a low-level southwesterly jet. Before the heavy precipitation process, there is large precipitable water content and deep warm clouds, which provides a potential for the occurrence and development of the heavy rainfall process in Longhua Town of Longmen County and its surrounding areas. Simultaneously, the low-level southwesterly jet provides abundant warm-wet water vapor for the heavy rainfall area. The vertical atmospheric environmental conditions, such as strong horizontal temperature gradient, high convective available potential energy, high-temperature difference between 850 hPa and 500 hPa, and low convective inhibition, maintain for a long duration in the heavy rainfall area, which are favorable for the occurrence and development of high-efficiency convective precipitation caused by water vapor condensation due to the uplift of low-level warm-wet airflows. The combined effects of the enhanced low-level southwesterly airflow, the stationary front, the mesoscale surface convergence line generated by cold pool outflows, the terrain influence, and the train effect of the precipitation echoes make heavy precipitation near Longhua last longer and stronger than other areas, leading to the extreme heavy rainfall with the record-breaking 3-h accumulated rainfall in Longhua.

Keywords: extreme heavy rainfall; low-level southwesterly jet; stationary front; South China

check for updates

Citation: Chen, F.; Li, H.; Hu, S.; Jiang, S.; Li, J.; Wu, R. Formation Mechanisms of the "5·31" Record-Breaking Extreme Heavy Rainfall Process in South China in 2021. *Atmosphere* **2023**, *14*, 872. https://doi.org/10.3390/atmos14050872

Academic Editor: Tomeu Rigo

Received: 23 April 2023
Revised: 10 May 2023
Accepted: 10 May 2023
Published: 16 May 2023

1. Introduction

Recently, extreme heavy rainfall events have occurred frequently in China, such as the "5·7" process in Guangzhou in 2017 with a record-breaking 3-h and 12-h accumulated amount of 382.6 and 542.7 mm, respectively, for Guangdong Province; the hourly rainfall rate of 184.4 mm h^{-1} at Yongning was close to the highest rate of 188 mm h^{-1} recorded at Yangjiang, Guangdong Province, on 23 June 2013 [1–3]. The "13·8" process in Gaotan of Huidong in 2013 with a record-breaking 24-h rainfall of 924.3 mm was observed for Guangdong Province [4,5]. The "18·8" extreme heavy rainfall process in 2018 with a record-breaking 24-h rainfall of 1056.7 mm over the "13·8"process occurred in the same place [6,7]. The "21·7" extreme heavy rainfall process in Zhengzhou of Henan Province in 2021 also took place, with accumulated precipitation of more than 1000 mm over a 6-day period that exceeded its mean annual precipitation [8–10]. These precipitation events have attracted great attention from meteorological forecasters and scholars, and have been interpreted and analyzed in numerous previous studies. The above-mentioned extreme heavy precipitation events show the same characteristics, such as intense short-term rainfall and long duration. However, the formation mechanisms of extreme heavy rainfall events vary in different regions at different time, and rainfall events have noticeable differences in influenced range, social impact, and disaster losses. Therefore, in order to better understand and grasp the formation mechanisms of local extreme heavy rainfall and further provide meteorological decision-making services for local disaster prevention and mitigation, it is essential to investigate the impact systems of extreme heavy precipitation processes and the evolution characteristics of their physical quantities.

The rainstorm center in northern Guangdong, located in the north of the Pearl River Delta and the south of the Nanling Mountains, is one of the three rainstorm centers in Guangdong [11]. Longmen County in the north of Huizhou is located in the central area of this rainstorm center. In Longmen, the maximum annual rainfall (2488.6 mm) and maximum rainstorm days (12.3 days) both appear in Nankunshan [12] in the west of Longmen. Rainstorms are the most serious meteorological disaster affecting Longmen. In particular, heavy rainfall occurs frequently during the first rainy season (April–June), since the 21st century, there have been two strong precipitation processes that broke Guangdong records. One is the continuous heavy rainfall process in South China ("05·6" process occurring on June 2005), with 7 continuous rainfall days in Longmen national weather station (3 continuous days of extraordinary heavy rain) and the 7-day accumulated precipitation of 1330.2 mm (the extreme value of rainfall in Guangdong Province). The other is the precipitation process from 0500–0800 CST on 31 May 2021, with the 3-h accumulated precipitation of 400.9 mm in Longhua of Longmen, breaking the historical record in Guangdong Province (382.6 mm in Zengcheng of Guangzhou from 0500–0800 CST on 7 May 2017).

Many scholars have thoroughly studied the diurnal variation characteristics [13], multi-scale influencing systems [14–17], and formation mechanisms [18,19] of heavy rainfall in South China. Moreover, the China Meteorological Administration (CMA) Longmen Field Experiment Base for Cloud Physics is jointly established by the Guangzhou Institute of Tropical and Marine Meteorology of the CMA and the Chinese Academy of Meteorological Sciences, in order to satisfy the demand for mechanism analysis of rainstorms in South China and the development of numerical forecast models [20]. At present, the research on the record-breaking extreme heavy rainfall in the rainstorm center in northern Guangdong mainly focuses on the "05·6" persistent heavy rainfall process. The "05·6" persistent heavy rainfall process is widely concerning due to the characteristics of its long duration, wide influenced range, and the large losses and severe disasters it causes. However, most studies about this process focused on analyzing its mechanisms in the perspective of large-scale and planetary-scale influencing systems [21–23]. In addition, some scholars have carried out diagnostic analyses and numerical simulations in the perspective of the mesoscale influencing systems [24,25]. The study areas of the above research were large, and the causes of maximum and extreme total rainfall in Longmen were not analyzed. Considering the extreme 3-h accumulated rainfall in Longhua of Longmen and relatively smaller area of heavy rainfall on 31 May 2021, which is somewhat different from the persistent heavy rainfall on June 2005, it is of interest to investigate the characteristics and causes of the extreme rainfall on 31 May 2021. Therefore, in this study, we investigate the "5·31" extreme heavy rainfall case in Longhua of Longmen in 2021. Specifically, the precipitation properties and formation mechanisms are analyzed in this research based on the synoptic analysis method. The research results are expected to improve the understanding of the causes of extreme heavy rainfall in Longmen of Huizhou, and assist the meteorological decision-making services of social disaster prevention, mitigation, and relief.

2. Data and Method

In this study, the method mainly used is the synoptic analysis method. The data used in this research include the ERA5 hourly global reanalysis data (the fifth generation European Center for Medium Range Weather Forecasts reanalysis), with a spatial resolution of $0.25^\circ \times 0.25^\circ$ and 37 vertical layers. The study period of this reanalysis data is from

30 May to 31 May 2021. In addition, the real-time observation data are applied to analyze the weather situation and physical qualities. The raindrop spectrum data of the DSG5 precipitation phenomenon instrument used in the operations of Longmen, the 3 km CAPPI radar mosaics from Guangdong weather radar, and the dual-polarization radar products in Heyuan are also used.

3. Overview of the "5·31" Precipitation Process

3.1. Spatio-Temporal Distribution Characteristics of the Rainfall

From the nighttime of 30 May to the daytime of 31 May 2021, precipitation echoes were generated and developed continuously in most parts of Guangdong along the coast of South China, especially in northern and eastern Guangdong. The most intensive precipitation echoes appeared from 0400–0800 CST on 31 May; the heavy rainfall area was mainly located within the northern-Guangdong rainstorm center. The characteristics of this process are prominent, mainly showing strong localization of heavy rainfall, obvious rainy night characteristics, severe short-term rainfall intensity, a large accumulated rainfall amount, and low strong centroid echoes.

From the spatial distribution of the rainfall (Figure 1a), it can be found that the local characteristics of this heavy rainfall are prominent. Before dawn on 31 May, the precipitation mainly appears in the area of northern–eastern Guangdong, and the heavy rainfall belt is distributed in a northwest–southeast pattern. The maximum rainfall center is located in Longmen County (the strongest heavy rainfall center) and eastern Boluo County (sub-center) of northern Huizhou.

The hourly rainfall variations (Figure 1b) indicate that this process is characterized by obvious rainy night, severe short-term rainfall intensity, and large accumulated rainfall amount. The precipitation mainly occurs from 0400–0800 CST. There are 17 weather stations in Longmen and Boluo Counties with accumulated rainfall exceeding 100 mm, accounting for about 35% of the total number of stations in the two counties. Additionally, there are two stations in Longmen County and Boluo County with rainfall exceeding 250 mm. The maximum rainfall appears at Longhua station, with a total amount of 462.3 mm, the hourly rainfall of the station exceeds 50 mm for 4 consecutive hours, the maximum 1-h rainfall reaching 156.4 mm (0600–0700 CST). Note that the accumulated rainfall from 0500–0800 CST reaches 400.9 mm, breaking the record of 3-h accumulated rainfall in Guangdong Province. In the heavy rainfall sub-center (eastern Boluo County), the maximum rainfall amount is 320.7 mm, appearing at the Mabei station in Boluo, with the maximum 1-h rainfall reaching 106.5 mm (0600–0700 CST).

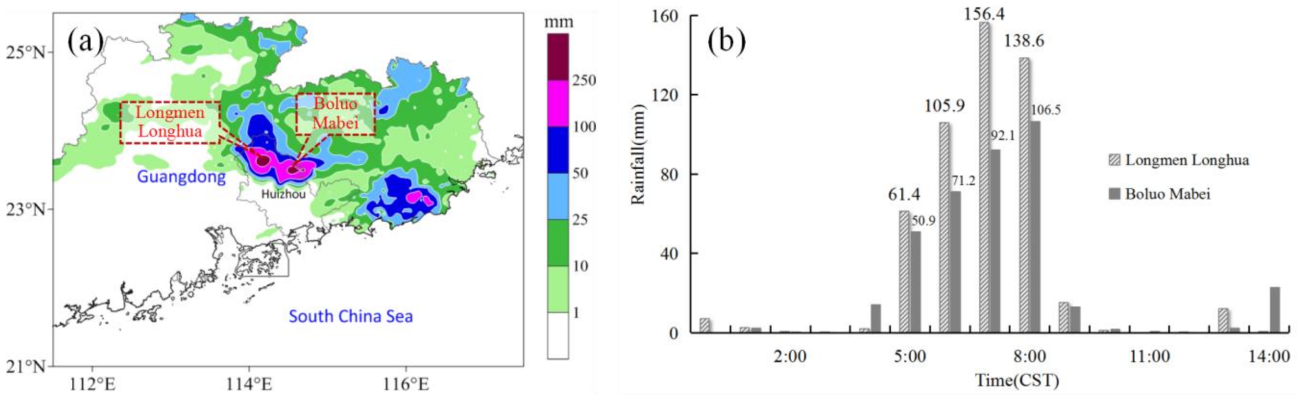

Figure 1. (**a**) Accumulated rainfall (mm) from 0400–0800 CST on 31 May 2021 in Guangdong Province, and (**b**) 1-h rainfall evolutions (mm) at Longhua station of Longmen and at Mabei station of Boluo.

The observation data of 10-m wind speed and lightning (figure omitted) show that the lightning is dense during this precipitation process, but the short-term gale is not obvious. There are only four weather stations in eastern Boluo with the maximum instantaneous wind speed reaching 10.8–17.9 m s^{-1} (0500–0800 CST), and none of the stations in Longmen observed the instantaneous wind speed reaching 10 m s^{-1}. The radar echo characteristics in the heavy rainfall area of northern Huizhou (Figure 2) suggest that the strongest composite reflectivity factor is about 60 dBZ, the height of strong echoes greater than or equal to 50 dBZ is basically lower than 5 km (figure omitted), and the height of echoes greater than or equal to 40 dBZ develops upwards to 10 km. The results indicate that this heavy rainfall process exhibits the characteristics of low centroid echoes. In addition, as shown in Figure 2c, during the strongest precipitation period from 0500–0800 CST, the reflectivity factor Z over Longhua is basically greater than or equal to 45 dBz, the differential reflectivity Z_{DR} is about 1 dB, and the differential phase shift rate K_{DP} is greater than or equal to 2 deg km^{-1}. The analysis indicates that the raindrop sizes of this process are average, but the raindrop concentration is high, displaying the characteristics of tropical heavy rainfall.

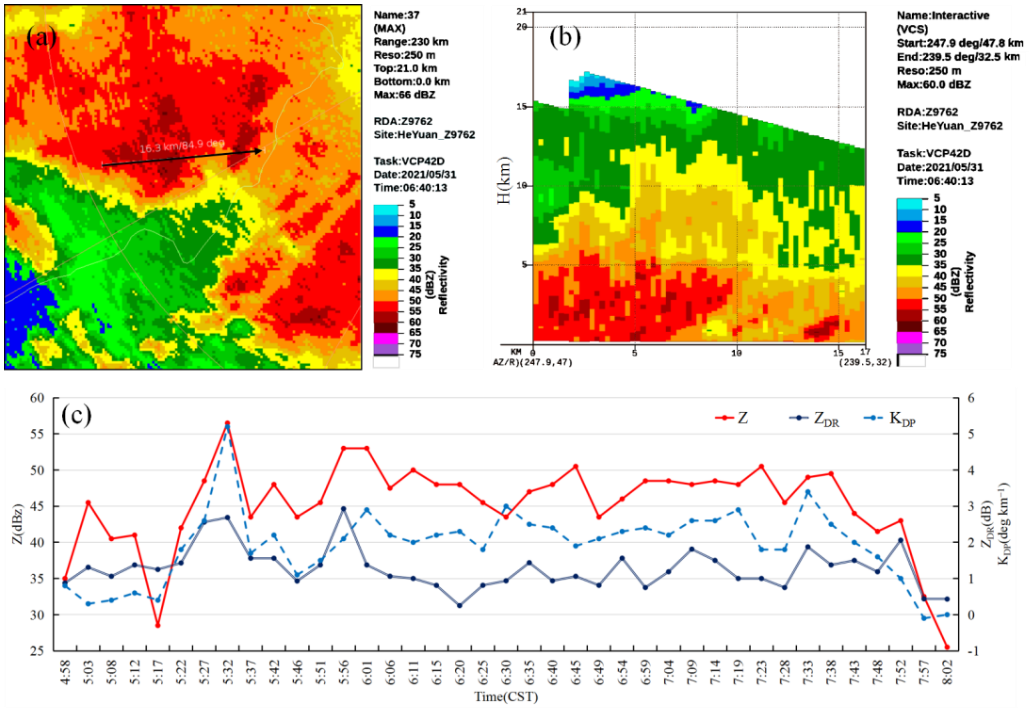

Figure 2. (**a**) Horizontal distribution and (**b**) vertical profile of the radar composite reflectivity at Heyuan station at 0640 CST on 31 May 2021, and (**c**) temporal evolutions of the reflectivity factor (Z), differential reflectivity (Z_{DR}), and differential phase shift rate (K_{DP}) at the 1° elevation angle in Longhua of Longmen from 0458–0802 CST. The black arrow in (**a**) represents the location and direction of the profile in (**b**).

Overall, this precipitation process is characterized by strong localization, obvious rainy night, severe short-term rainfall intensity, large accumulated rainfall amount, not obvious short-term gale, and low centroid strong echoes. Additionally, this process was accompanied by pronounced thunderstorms, the radar echoes show the characteristic of tropical heavy rainfall.

3.2. Atmospheric Circulation Characteristics

At 2000 CST on 30 May (before the heavy rainfall), the western Pacific subtropical high was distributed in an east-west belt, and the 588 dagpm line was located in the southern part of South China. The main influencing systems over eastern Guangdong are the south branch trough, the low-level shear line (Figure 3a), and the surface stationary front (Figure 3b) maintaining for a long time. As shown in the visible cloud images from 30 to 31 May (figure omitted), there is a band-shaped stationary front cloud system from the northeastern side of Japan to the southeast of China.

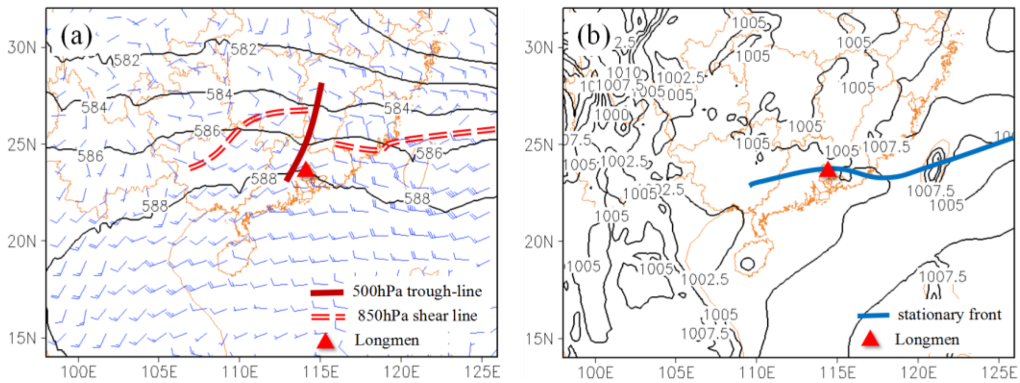

Figure 3. (**a**) Shows 500 hPa geopotential height (contours; interval: 2 dagpm) and 850 hPa wind field (wind barbs) at 2000 CST on 30 May 2021, and (**b**) sea level pressure (contours; interval: 2.5 hPa).

From 2000 CST on 30 May to 0800 CST on 31 May, the evolution of each weather system is mainly as follows. The upper-level divergence area at 200 hPa moves southward, and the east of the Pearl River Estuary is in the divergence area (figure omitted). The weak shortwave trough at 500 hPa in the middle level slowly moves eastward. The low-level shear line basically maintains or slightly moves southward. The most obvious variation is that the southwesterly wind at 850 hPa and 925 hPa strengthens from the Indochina Peninsula to central and eastern Guangdong (Table 1). By 0800 CST on 31 May, the 850 hPa wind speed at Yangjiang, Qingyuan and Hong Kong sounding stations increases to 12 m s^{-1}, reaching the intensity of jets. In addition, the 925 hPa wind speed at these stations increases to 8–10 m s^{-1}. However, at Heyuan station, the 850 hPa wind speed remains unchanged, and the 925 hPa wind speed increases from 1 m s^{-1} to 6 m s^{-1}, still remarkably smaller than that at the other three stations. From a comprehensive analysis of the vertical evolution of the wind field near the heavy rainfall area and its upstream wind profile radar products in Zengcheng of Guangzhou (figure omitted), it can be seen that the effect of the 850 hPa low-level jet over the heavy rainfall area is more obvious. Combined with the horizontal divergence field and wind field at 850 hPa (Figure 4), we found that there is a clear convergence zone at the front of the low-level southwesterly jet axis. Moreover, the convergence area moves northeastward with the enhancement of the low-level southwesterly jet before the dawn of 31 May, affecting the heavy rainfall area. That is, the low-level convergence is formed in the front of the enhanced low-level southwesterly jet, which is conducive to the occurrence and development of the heavy rainfall process in Longhua of Longmen and the surrounding areas.

Table 1. Wind speed (m s^{-1}) at Guangdong sounding stations from 2000 CST on 30 May to 0800 CST on 31 May 2021.

Stations		**2000 CST on 30 May**	**0200 CST on 31 May**	**0800 CST on 31 May**
Yangjiang	850 hPa	9.6	9.4	12.1
	925 hPa	7.6	6.8	8.1
Qingyuan	850 hPa	7.0	8.0	12.0
	925 hPa	3.0	6.0	8.0
Hong Kong	850 hPa	6.0	7.0	12.0
	925 hPa	5.0	9.0	10.0
Heyuan	850 hPa	5.0	-	5.0
	925 hPa	1.0	-	6.0

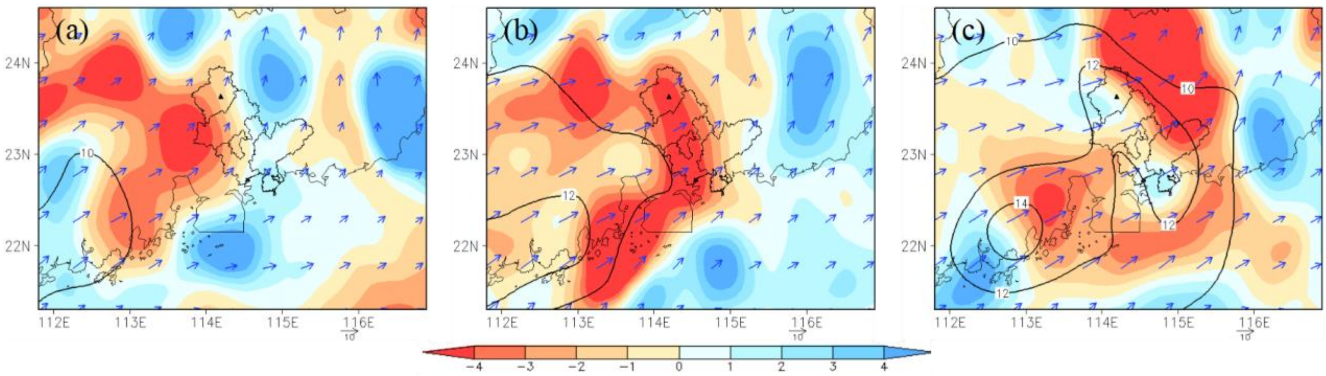

Figure 4. Wind field at 850 hPa (wind barbs, contours represent the wind speed above 10 m s^{-1}) and divergence field (shaded areas; interval: 1×10^{-5} s^{-1}) at (**a**) 0200 CST, (**b**) 0500 CST, and (**c**) 0800 CST on 31 May 2021. The black triangle in (**a**–**c**) represents the location of Longhua, Longmen.

Hence, the low-level southwesterly jet strengthens the rainfall intensity in northern Huizhou under the dynamic uplifting effect of the weather systems such as weak upper-level shortwave trough and surface stationary front. Under the favorable synoptic-scale atmospheric circulation background, it is necessary to explain the causes of the high precipitation efficiency and the long duration of the heavy rainfall process in Longhua, Longmen from the aspects of small- and meso-scale weather systems.

4. Formation Mechanism of the Extreme Heavy Rainfall in Longhua of Longmen

Doswell III et al. [26] found that the precipitation factors triggering flash floods depend on the intensity and duration of precipitation. Sun et al. [27] pointed out that rainfall amount is determined by water vapor content in the atmosphere and condensation efficiency and duration. Yu et al. [28] also indicated that the identification of short-term heavy rainfall events is mainly based on rainfall intensity and duration, and rainfall intensity depends on the combined effect of precipitation efficiency, updraft velocity at cloud bottom, and specific humidity. Thus, in this study, the formation mechanisms of the extreme heavy rainfall lasting for about 4 h in Longhua of Longmen is analyzed from the aspects of water vapor conditions, condensation efficiency, and duration.

4.1. Abundant Water Vapor Conditions

The water vapor conditions include the distribution of water vapor content and water vapor transport [28]. Water vapor content can be analyzed by the quantities such as specific humidity, precipitable water content, and warm cloud thickness. Water vapor transport can be interpreted by water vapor flux and water vapor flux divergence.

From 2000 CST on 30 May to 0200 CST on 31 May (before the heavy rainfall), the physical qualities at Heyuan sounding station near Longhua of Longmen (Figure 5) illustrate that the wet layer in lower levels is thick, but the middle troposphere is relatively dry, i.e., the troposphere shows a vertical distribution characteristic of "dry at upper levels and wet at low levels". The 850 hPa specific humidity reaches 13–15 g kg^{-1}, exceeding the specific humidity threshold of severe convective weather in Guangdong (12 g kg^{-1}). The precipitable water content reaches 50–65.7 kg m^{-2}, and the warm cloud layer is deep, with a thickness of 4327.7–4517.6 m. Both quantities exceed the multi-year average values in May–June at this station (the average values of precipitable water content and warm cloud layer thickness are 51.2 kg m^{-2} and 4198.5 m in May–June from 2010 to 2022, respectively). The results indicate that before the heavy precipitation, stratification over the area near Longhua of Longmen is unstable, there are favorable conditions prone to heavy rainfall such as precipitable water content, and deep warm cloud layer thickness.

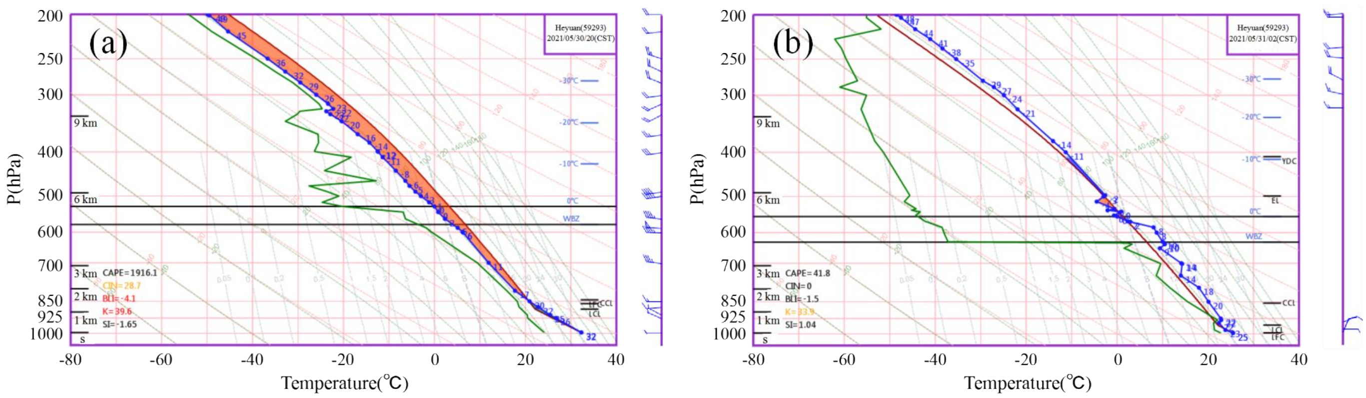

Figure 5. The T-lnP diagrams from Heyuan sounding station (dew point temperature stratification curve in green, temperature stratification curve in blue and state curve in red) at (**a**) 2000 CST on 30 May and (**b**) 0200 CST on 31 May 2021.

The abundant water vapor supply is the necessary condition for the occurrence and development of extreme heavy precipitation. During this precipitation process, the pulse of the southwesterly jet not only enhances the dynamic uplifting effect in the heavy rainfall area, but also provides sufficient water vapor for the occurrence and development of heavy rainfall. At the same time, the water vapor convergence in the front of the jet enhances the rainfall intensity in this region. As shown in Figure 6a–d, the large-value area of water vapor flux convergence advances continuously with the southwesterly monsoon jet at 850 hPa. Moreover, there is a high-value area of water vapor flux convergence maintaining in northern Huizhou from 0500–0800 CST, which obviously moves to the eastern side of Longmen at 1100 CST. From the relative humidity observations at the stations on the west (Paitan station in Zengcheng) and east (Longcheng station in Longmen) sides of Longhua (Figure 6e), it can be found that the relative humidity at the western station gradually increases to 95% and above after 2200 CST on 30 May and gradually reduces after 0600 CST on the morning of 31 May. In contrast, the relative humidity at the eastern station increases relatively later and maintains a high value after 0100 CST on 31 May. The real-time observations are consistent with the temporal evolution of the water vapor calculated by the reanalysis data, suggesting that the high-value area of water vapor flux convergence appears in the front of the low-level southwesterly jet. With the northeastward development of the southwesterly jet, the favorable water vapor conditions for the heavy rainfall in northern Huizhou before the dawn of 31 May are generated.

In conclusion, there were favorable conditions for high precipitation efficiency, which included deep warm cloud layer thickness and precipitable water content in the whole layer before the heavy rainfall. Meanwhile, the enhancement of the low-level southwesterly jet provides abundant water vapor for the heavy rainfall area, satisfying the water vapor conditions for the occurrence and development of the extreme heavy rainfall.

4.2. High Efficiency of Water Vapor Condensation

Condensation efficiency during precipitation processes is determined by the relative temperature difference between air masses, i.e., temperature gradient. Horizontal temperature gradient is one of the main factors determining dynamic forced uplifting, and the uplifting forced by warm advection is the basic reason for water vapor condensation. Vertical temperature gradient is one of the main factors determining the convective available potential energy (CAPE) [27].

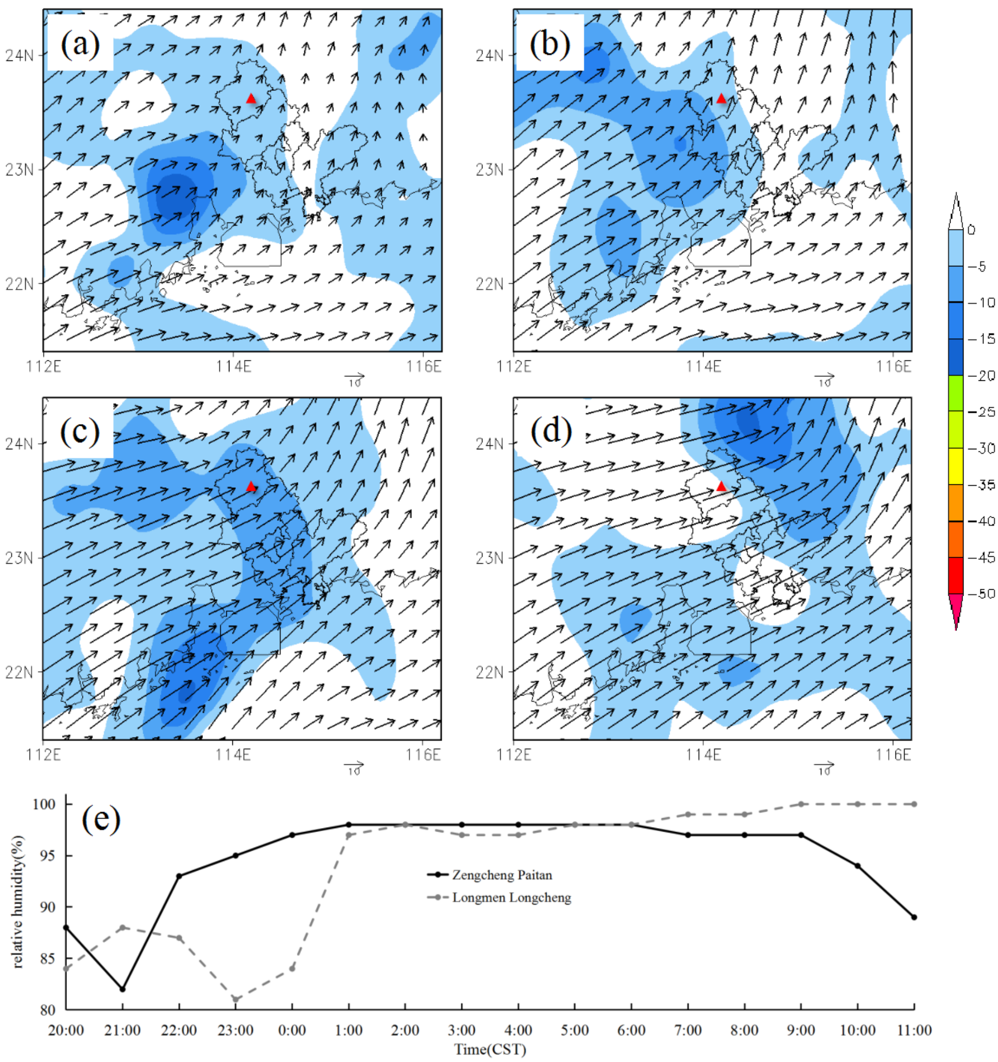

Figure 6. Water vapor flux (vector) and water vapor flux divergence (shaded areas; 10^{-8} g cm^{-2} hPa^{-1} s^{-1}) at (**a**) 2300 CST on 30 May and at (**b**) 0200 CST, (**c**) 0500 CST, and (**d**) 0800 CST on 31 May 2021, and (**e**) the evolutions of relative humidity at Paitan and Longcheng stations from 2000 CST on 30 May to 1100 CST to 31 May 2021. The red triangles in (**a**–**d**) represent the location of Longhua of Longmen.

Through the analysis of the evolution characteristics of 2-meter horizontal temperature at weather stations (Figure 7), it can be seen that after 0200 CST on 31 May, with the increase in the low-level southwesterly wind speed, a warm tongue extends northeastward in Huizhou and maintains for a long time. The temperature within the warm tongue maintains or rises. Specifically, the temperature increases from 26.5 °C at 0400 CST to 29.0 °C at 0700 CST at Mabei station 30 km away from the southwest of Longhua. Due to the influence of the cold pool caused by precipitation, the temperature at the stations on the northeast side of Longhua maintains or decreases in the early morning of 31 May, and it is about 24 °C during 0600–0800 CST. Therefore, the temperature difference between the northeast and southwest sides of Longmen County gradually increases, and there is an obvious northwest–southeast horizontal temperature gradient belt. The maximum temperature difference between both sides of the temperature gradient belt reaches 5 °C, i.e., about 2.5 °C (10 km)$^{-1}$, slightly smaller than the horizontal temperature gradient of 3.3–3.5 °C (10 km)$^{-1}$ in “18·8” extreme heavy rainfall process with 24-h accumulated precipitation of 1056.7 mm in Gaotan of Huidong. The strong horizontal temperature gradient can force a remarkable increase in local vertical wind shear [7], which is conducive to the uplifting condensation of low-level warm and wet water vapor.

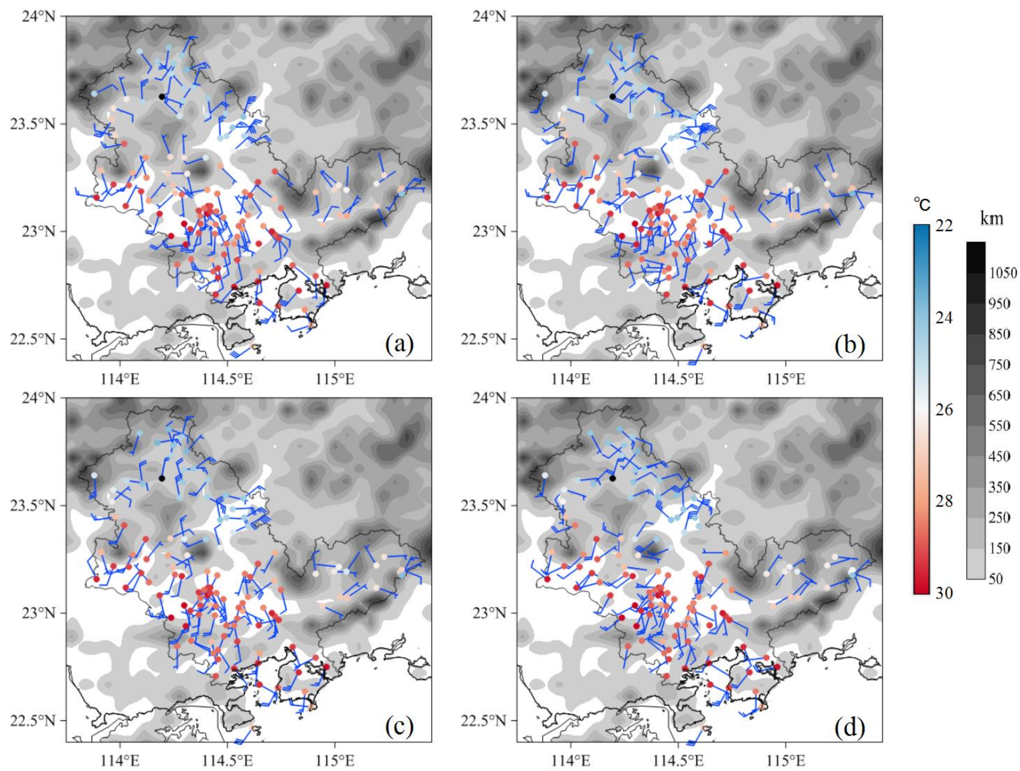

Figure 7. The 2-meter temperature (dots), 10-meter wind field (wind barbs), and altitudes (shaded areas) at the weather stations in Huizhou from 0500 CST (**a**), 0600 CST (**b**), 0700 CST (**c**) and 0800 CST (**d**) on 31 May 2021. The black dots in (**a**–**d**) represent the location of Longhua station in Longmen.

During convective precipitation processes, CAPE values are proportional to the rising speed of the cloud base [28]. Sun et al. [27] pointed out that when the low-level water vapor is forced to lift above the condensation height due to the horizontal convergence of flow field, water vapor condensation may occur, and precipitation may appear due to the condensation. When water vapor is further lifted above the convective condensation height, a convection phenomenon may occur. Convective processes are often accompanied by intense upward motion. If the condensation rate is the product of the upward speed and condensation function, the stronger the convective activities are, the greater the precipitation intensity is. During this precipitation process, at 2000 CST on 31 May, the temperature difference between 850 hPa and 500 hPa ($\Delta T_{85\text{–}50}$) at Heyuan sounding station is 24 °C (Figure 5), reaching the convection threshold in Guangdong Province. The CAPE value is 1916.1 J kg^{-1}, exceeding the average CAPE in May–June from 2010 to 2022 (702.6 J kg^{-1}). Additionally, the CIN value is 28.7 J·kg^{-1}, which is lower than the average CIN in May–June from 2010 to 2022 (51.2 J kg^{-1}) at this station. By 0200 CST on 31 May, the CAPE and CIN values are not available due to one precipitation event already occurring at the station, but the $\Delta T_{85\text{–}50}$ still is 23 °C. Therefore, the vertical atmospheric environment conditions have high water vapor condensation efficiency, which favors the occurrence and development of short-term heavy rainfall near Longhua of Longmen, and even extreme heavy rainfall.

The synoptic-scale vertical velocity and divergence fields also indicate that there is strong upward motion over the heavy rainfall area. As shown in Figure 8, the negative vertical velocity area south of 23.5° N gradually moves northeastward with the southwesterly jet. From 0500–0800 CST on 31 May, the intensity of vertical upward motion near Longmen of Longhua is the strongest. Meanwhile, the low-level convergence over this region also strengthens. At 0800 CST, a typical circulation situation of low-level convergence and upper-level divergence is established. The strong upward motion and the vertical circulation configuration of low-level convergence and high-level divergence are favorable for the forced uplifting of warm and wet water vapor in the lower levels to above the convective condensation height, which further favors the development of short-term heavy rainfall.

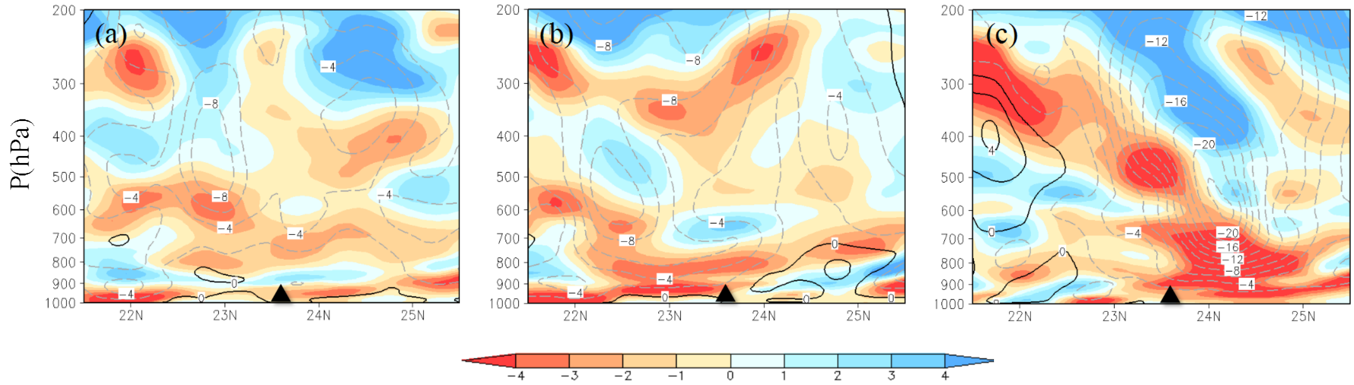

Figure 8. Pressure-latitude sections of the vertical velocity (contours; 10^{-1} Pa s^{-1}) and divergence (shaded areas; interval: 1×10^{-5} s^{-1}) averaged in the range of 114° E–115° E at (**a**) 0200 CST, (**b**) 0500 CST, and (**c**) 0800 CST on 31 May 2021. The black triangles in (**a**–**c**) represent the location of Longhua in Longmen.

Raindrop spectra are an essential parameter in cloud precipitation physics [29]. Therefore, we analyze the raindrop spectrum distribution characteristics from the DSG5 precipitation phenomenon instrument in Longmen national weather station (Figure 9), which is near the heavy precipitation area. From 0400–0800 CST, the hourly raindrop spectra show the same variation trend, with a larger raindrop spectral width. The maximum particle size can reach 7–8 mm. In addition, the greater the rainfall intensity, the greater the particle size and number concentration. This result is consistent with the characteristics of convective precipitation. The raindrop spectra exhibit a single-peak distribution, and when the particle size is 0.625–0.75 mm, the particle number concentration is the highest, consistent with the characteristics of the differential reflectivity and differential phase shift rate of the dual-polarization radar in Section 3.1. Compared with the average raindrop spectrum during May–June from 2017 to 2020 (gray dash line in Figure 9b), we find that the distribution of the average raindrop spectrum from 0400–0800 CST in this process (black dash line in Figure 9b) is similar, but the number concentration of particles with a diameter less than 7 mm is obviously larger during this process. Moreover, due to the small range of extreme heavy rainfall in this process (about 10 km radius from Longhua), Longmen national weather station, about 18 km away from the northeast of Longhua of Longmen, has a remarkably weaker rainfall intensity than that in Longhua of Longmen. Therefore, the situation with rainfall intensity above 100 mm h^{-1} (red dash line in Figure 9b) is selected for the composite in order to better match the characteristics of the raindrop spectra near Longhua in this process. The results show that the spectrum distribution is similar, but the particle number concentration is far higher than at the time with weaker rainfall intensity, indicating that the rainfall process is a convective precipitation process with a large raindrop spectrum width. The higher the particle number concentration, the stronger the rainfall intensity.

In summary, during the heavy rainfall process, the large horizontal temperature gradient near Longhua of Longmen is conducive to the uplifting of low-level warm and wet water vapor. In addition, the vertical atmospheric environmental conditions of the high CAPE, high ΔT_{85-50}, and low CIN are favorable for high precipitation condensation efficiency, which facilitates the occurrence and development of short-term heavy rainfall and even extreme heavy rainfall near Longhua of Longmen.

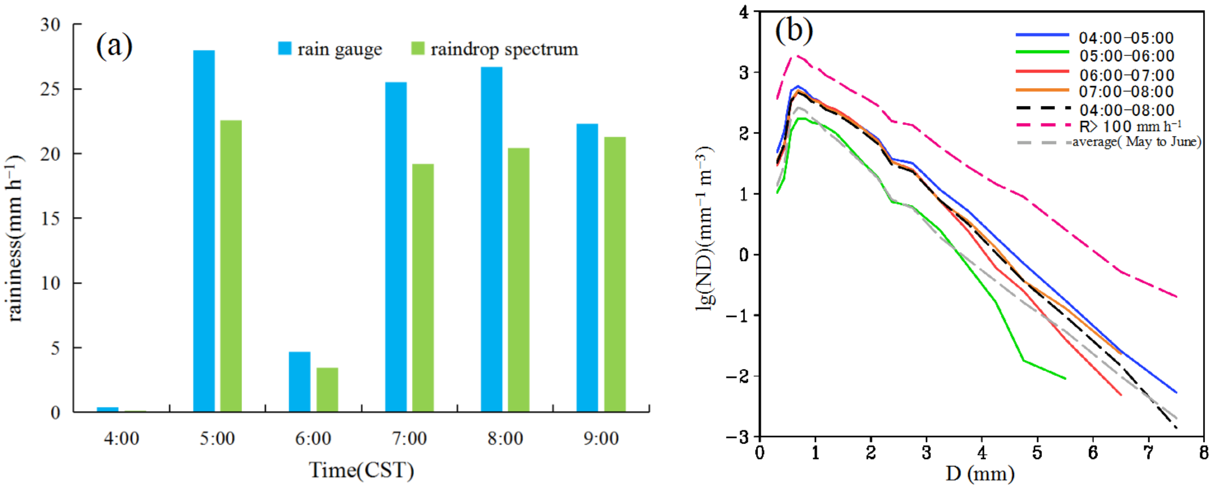

Figure 9. (**a**) The comparison of the rainfall intensity between the station observations and inversions by the raindrop spectra at Longmen national weather station from 0400–0800 CST on 31 May 2021, and (**b**) the distribution characteristics of the raindrop spectra.

4.3. Causes of the Long Duration of This Heavy Rainfall Process

This extreme heavy rainfall process in Longhua of Longmen occurred under the joint effect of favorable atmospheric circulations, including the weak middle-level shortwave trough, the surface stationary front, and the low-level southwesterly jet. Meanwhile, due to the terrain effect, the interactions of the cold pool generated by precipitation and the enhanced southwesterly jet on the eastern side of Longmen County (the northeastern side of the heavy rainfall area) play a crucial role in the long duration of heavy rainfall in Longhua.

4.3.1. Effects of the Mesoscale Surface Convergence Line

According to the analysis in Section 4.2, it can be found that there is a northwest–southeast horizontal temperature gradient belt maintaining for a long time near Longhua. Based on the 10-meter wind field from the weather stations in Figure 7, we find that there is a remarkable difference in wind direction on both sides of the temperature gradient belt. An obvious mesoscale surface convergence line is formed between the southwesterly wind in the warm section on the southwest side and the easterly wind in the cold section on the northeast side, and this convergence line maintains from 0500–0800 CST. With the enhancement of the low-level southwesterly jet, the surface wind speed on the southwest side of Longhua also increases at 0300 CST and remains relatively large during 0600–0800 CST, but the extreme maximum wind speed does not exceed 10 m s^{-1}. The same variation characteristics also can be found in the northeasterly and easterly wind in the low-temperature area of Longhua and its northeast side. In other words, the surface mesoscale convergence line strengthens during the heavy rainfall process. Combined with the location of the stationary front in Figure 3b, we find that the position of the stationary front roughly coincides with the surface mesoscale convergence line. The combined effect of the two systems is more conducive to the occurrence, development, and maintenance of the heavy rainfall.

Moreover, the topographic distribution is also taken into consideration. Longmen in Huizhou is located on the northeast side of the Pearl River Delta, and its terrain declines from the northwest to the southeast, with high mountains in the northwest and southwest, and low hills and basins in the east and south. Longhua is located on the west side of the region with low hills and basins. The relatively low-temperature area with a temperature of about 24 °C is mainly located in the region with low hills and basins, resulting in the outward expansion of cold pool outflows to slow down or stagnate, and leading to the northeasterly and easterly airflows in the low-temperature area maintaining for a long time.

As the enhanced low-level southwesterly warm and wet airflow moves to the edge of the low-temperature area, the high-value area of the horizontal temperature gradient belt and the surface mesoscale convergence line is maintained and strengthened, i.e., the terrain has an effect on the maintenance of the mesoscale surface convergence line.

Overall, the combined effects of the enhanced low-level southwesterly jet, the mesoscale surface convergence line generated by the cold pool outflows, the stationary front, and the terrain of low hills and basins on the north side of Longhua of Longmen resulted in the heavy rainfall remaining longer and stronger than in other regions, favoring the extreme heavy rainfall with record-breaking 3-h accumulated precipitation in Longhua.

4.3.2. Train Effect of Multi-Cell Storms

When the enhanced low-level southwesterly warm and wet airflow moves to the stationary front and surface convergence line, the radial velocity maps of dual-polarization radar at Heyuan station (Figure 10) show that a weak convergence area is gradually formed in the west of Longhua and lasts for a long time. It causes initial convection to be triggered continuously in Nankunshan on the northeast side of the Pearl River Delta. The initial convection subsequently strengthens and moves eastward under the impact of steer flows. The radar echo maps show that there are precipitation echoes continuously passing through Longhua and its surrounding areas, which is a remarkable phenomenon of the train effect (Figure 11). The train effect of precipitation echoes is favorable for the long duration of heavy rainfall. By numbering the convective cells or multi-cell storms influencing Longhua and surrounding areas (Figure 11), it can be seen that there are roughly three multi-cell storms (A, B, and C) passing through the heavy rainfall area, where the multi-cell storm C has the longest influencing duration (0500–0800 CST).

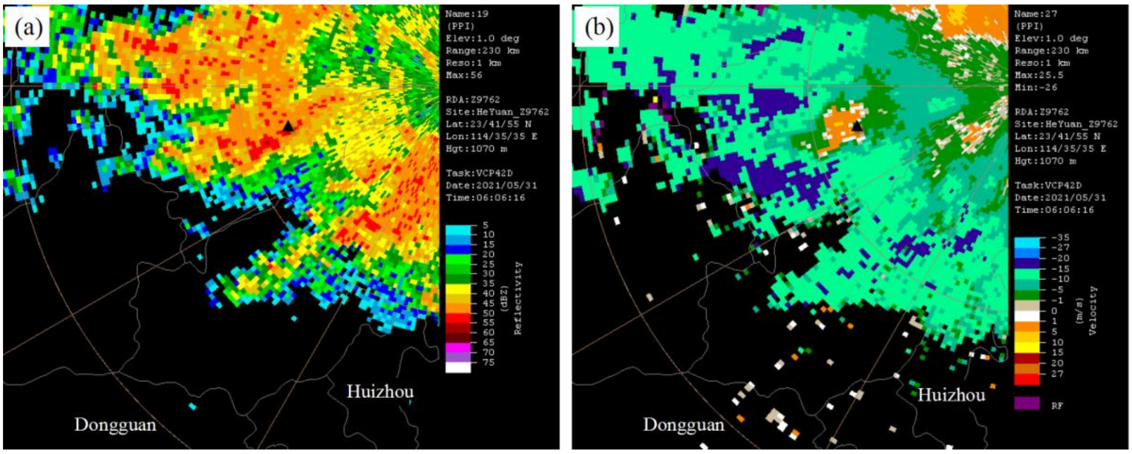

Figure 10. (**a**) Radar reflectivity factor and (**b**) radial velocity at Heyuan station at 0606 CST on 31 May 2021. The black triangles in (**a**,**b**) represent the location of Longhua station of Longmen.

Sun et al. [30] pointed out that the train effect generally occurs in unstable stratification in low-level warm sections and propagates along distinct airflows or low-level jets. Once the train effect appears, the maximum convective precipitation center generally appears in front of the propagation direction where there is also the high-value area of pseudo equivalent potential temperature (θ_{se}) gradient. Therefore, the formation mechanisms of the train effect in this rainfall process can be analyzed based on the evolution of θ_{se}. The vertical profile of θ_{se} in the heavy rainfall area (figure omitted) illustrates that the high-value area of θ_{se} is mainly concentrated in 950–850 hPa. Therefore, we analyze the evolution characteristics of θ_{se} at the most remarkable level of 900 hPa (Figure 12). The results indicate that the high-value belt of θ_{se} is consistent with the trend in the low-level southwesterly jet in Figure 4, extending in a southwest–northeast pattern. The dense area of the contours of θ_{se} is formed on the northeast side of the Pearl River Delta, which is also the high-value area of θ_{se} gradient. In the high-value area, the θ_{se} difference between

600 hPa and 900 hPa ($\Delta\theta_{se}$) is negative, revealing that θ_{se} decreases with height. Therefore, the atmosphere in the large-value area of θ_{se} gradient is in the baroclinic instability state, the initial convection is continuously triggered and developed in the region, resulting in the train effect of precipitation echoes. Longhua of Longmen is located in the high-value area of θ_{se} gradient, and thus it becomes the maximum heavy rainfall center in this process. Overall, the train effect favors the extreme heavy rainfall with the record-breaking 3-h accumulated precipitation in Longhua of Longmen.

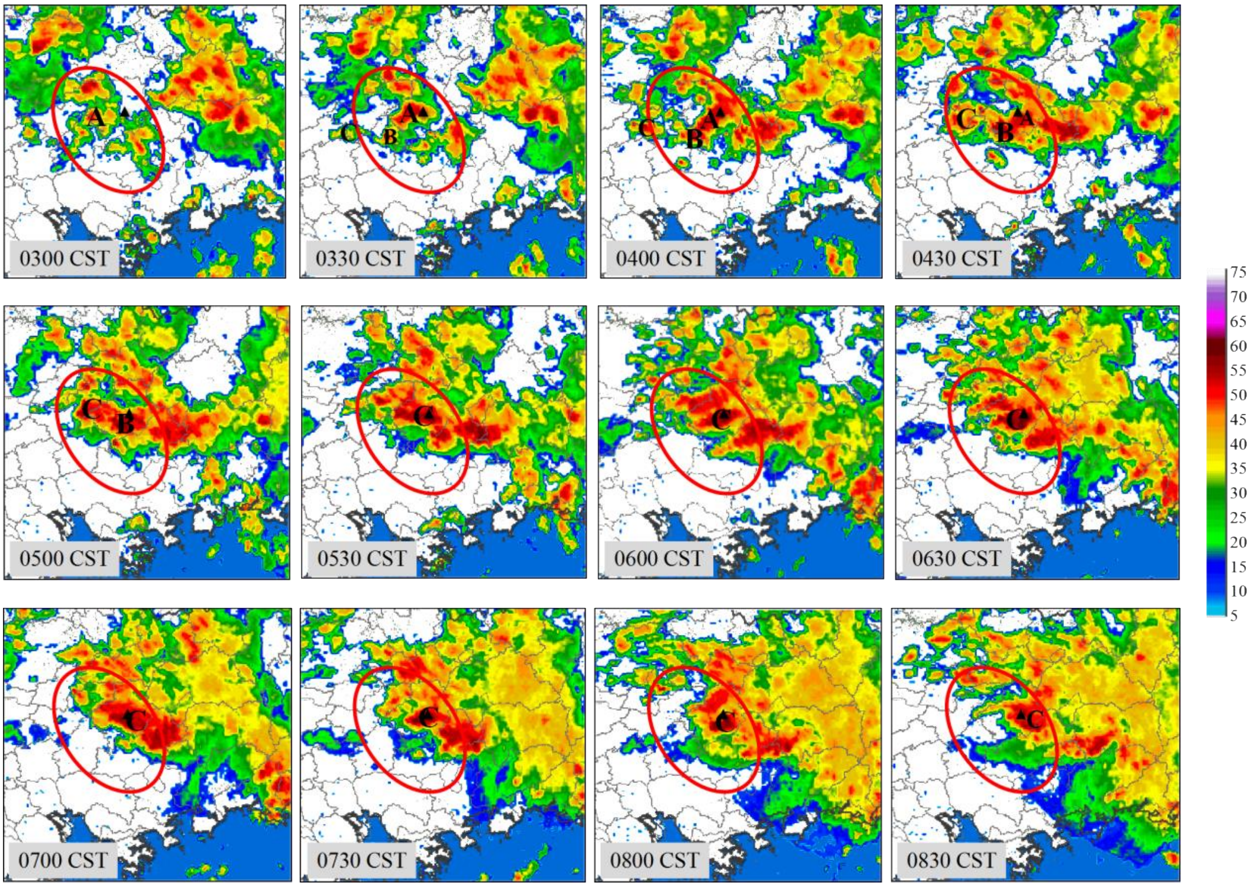

Figure 11. Radar echoes from 0300–0800 CST on 31 May 2021. A, B and C represent multi-cell storms. The black triangles represent the location of Longhua station, and the areas of focus are circled in red.

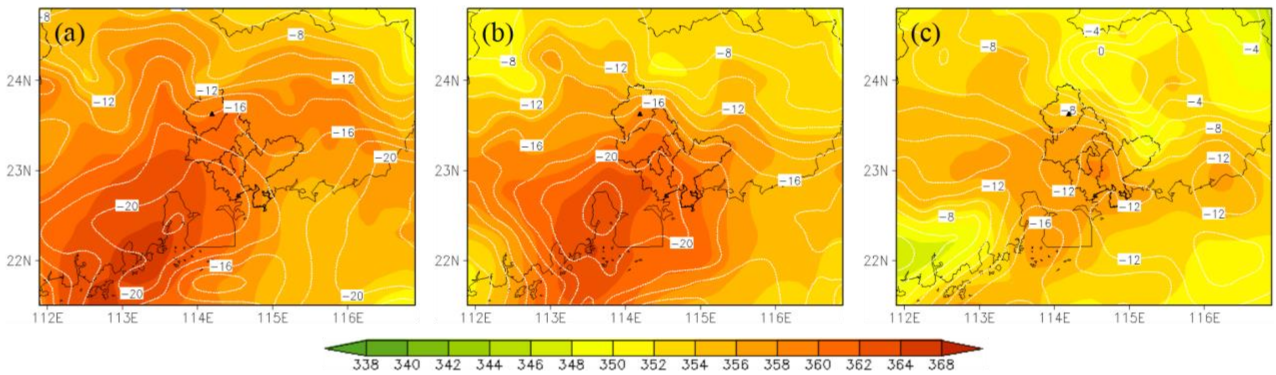

Figure 12. The pseudo-equivalent potential temperature at 900 hPa (shaded areas, interval: 2 K) and the difference of the pseudo-equivalent potential temperature between 600 hPa and 900 hPa (contours, interval: 2 K) at (**a**) 0200 CST, (**b**) 0500 CST, and (**c**) 0800 CST. The black triangles in (**a**–**c**) represent the location of Longhua station.

5. Conclusions

In this extreme heavy rainfall process with record-breaking 3-h accumulated precipitation in South China, the main influencing systems are a weak shortwave trough, a surface stationary front, and a low-level southwesterly jet. In terms of the formation mechanisms of this extreme heavy rainfall, the main conclusions are as follows.

Under the influences of the weak upper-level shortwave trough, surface stationary front, and low-level southwesterly jet, this precipitation process is characterized by strong localization, obvious rainy night, severe short-term rainfall intensity, and large accumulated rainfall amount. The radar echoes present the characteristics of tropical heavy rainfall with low centroid echoes.

Before the heavy precipitation, there is large precipitable water content and deep warm clouds near Longhua of Longmen, which provide a potential for the occurrence and development of heavy rainfall. Additionally, the enhancement of the low-level southwesterly jet provides abundant warm and humid water vapor for the heavy rainfall area, satisfying the water vapor conditions for the occurrence and development of extreme heavy rainfall.

During the heavy rainfall process, large horizontal temperature gradients appear near Longhua of Longmen, and the vertical atmospheric environmental conditions of the high CAPE, high ΔT_{85-50}, and low CIN are favorable for the uplifting and condensation of warm-wet water vapor at lower levels near Longhua of Longmen. Such conditions result in high water vapor condensation efficiency, thus causing short-term heavy rainfall and even extreme heavy rainfall.

The heavy rainfall near Longhua is under the joint actions of the stationary front, the mesoscale surface convergent line generated by the enhancement of the low-level southwesterly airflow and the cold pool outflows, the terrain of low hills and basins, and the train effect of the precipitation echoes. Therefore, its duration is longer, and its intensity is stronger compared with other areas, leading to the extreme heavy rainfall with the record-breaking 3-h accumulated precipitation in Longhua.

Therefore, in practical forecasting operations, when it is determined that a stable synoptic scale system (such as surface stationary front) is maintained for a long time and other favorable weather systems (such as high trough) exist for precipitation, the precipitation time, intensity, and area are closely related to the time, intensity, and wind direction changes of the enhancement of warm and humid air flow in the lower troposphere. Combining the increasing effect of terrain and other factors on precipitation can help to predict and provide services for (extreme) heavy rainfall.

Author Contributions: Conceptualization, F.C. and S.H.; Data curation, S.J., J.L. and R.W.; Formal analysis, F.C. and H.L.; Methodology, S.H. and S.J.; Validation, S.H. and H.L.; Writing—original draft, F.C., J.L. and R.W.; Writing—review and editing, J.L. and R.W. All authors have read and agreed to the published version of the manuscript.

Funding: This work was jointly supported by the National Natural Science Foundation of China (Grant No. U22422203, 42030610, 41975138, 42275008 and 42205012), the Science and Technology Development Fund Project of Guangdong Meteorological Bureau (Grant No. GRMC2021M23 and GRMC2021M25), the Guangdong Basic and Applied Basic Research Foundation (Grant No. 2021A1515011415), the Joint Research Project for Meteorological Capacity Improvement (Grant No. 22NLTSQ003).

Institutional Review Board Statement: Not applicable.

Informed Consent Statement: Not applicable.

Data Availability Statement: Not applicable.

Conflicts of Interest: The authors declare no conflict of interest.

References

1. Huang, Y.J.; Liu, Y.B.; Liu, Y.W.; Li, H.Q.; Jason, C.K. Budget analyses of a record-breaking rainfall event in the coastal metropolitan city of Guangzhou, China. *J. Geophys. Res. Atmos.* **2019**, *124*, 9391–9406. [CrossRef]
2. Li, M.X.; Luo, Y.L.; Zhang, D.L.; Chen, M.X.; Wu, C.; Yin, J.F.; Ma, R.Y. Analysis of a record-breaking rainfall event associated with a monsoon coastal megacity of south china using multisource data. *IEEE Trans. Geosci. Remote Sens.* **2020**, *59*, 6404–6414. [CrossRef]
3. Yin, J.F.; Zhang, D.L.; Luo, Y.L.; Ma, R.Y. On the extreme rainfall event of 7 May 2017 over the coastal city of Guangzhou. Part I: Impacts of urbanization and orography. *Mon. Wea. Rev.* **2020**, *148*, 955–979. [CrossRef]
4. Meng, W.G.; Wang, Y.Q. A diagnostic study on heavy rainfall induced by landfalling Typhoon Utor (2013) in South China: 1. Rainfall asymmetry at landfall. *J. Geophys. Res. Atmos.* **2016**, *121*, 12781–12802. [CrossRef]
5. Liu, L.; Xu, J.; Wang, Y.Q.; Duan, Y.H. Contribution of recycling of surface precipitation to landfalling tropical cyclone rainfall: A modeling study for Typhoon Utor (2013). *J. Geophys. Res. Atmos.* **2019**, *124*, 870–885. [CrossRef]
6. Li, H.Q.; Wan, Q.L.; Peng, D.D.; Liu, X.T.; Xiao, H. Multiscale analysis of a record-breaking heavy rainfall event in Guangdong, China. *Atmos. Res.* **2020**, *232*, 104703. [CrossRef]
7. Zeng, Z.L.; Chen, Y.; Wang, D.H. Observation and mechanism analysis for a record-breaking heavy rainfall event over Southern China in August 2018. *Chin. J. Atmos. Sci.* **2020**, *44*, 695–715. (In Chinese)
8. Chen, G.; Zhao, K.; Lu, Y.H.; Zheng, Y.Y.; Xue, M.; Tan, Z.M.; Xu, X.; Huang, H.; Chen, H.N.; Xu, F.; et al. Variability of microphysical characteristics in the "21·7" Henan extremely heavy rainfall event. *Sci. China Earth Sci.* **2022**, *10*, 1861–1878. [CrossRef]
9. Luo, Y.H.; Du, Y. The Roles of Low-level Jets in "21·7" Henan extremely persistent heavy rainfall event. *Adv. Atmos. Sci.* **2023**, *40*, 350–373. [CrossRef]
10. Wei, P.; Xu, X.; Xue, M.; Zhang, C.Y.; Wang, Y.; Zhao, K.; Zhou, A.; Zhang, S.S.; Zhu, K.F. On the key dynamical processes supporting the 21.7 Zhengzhou record-breaking hourly rainfall in China. *Adv. Atmos. Sci.* **2023**, *40*, 337–349. [CrossRef]
11. Lin, L.X.; Feng, Y.R.; Huang, Z.; Zeng, C.; Wu, Z.F.; Liu, Y.C.; Zeng, Q. *Technical Manual of Weather Forecast in Guangdong Province*; Meteorol Press: Beijing, China, 2006; pp. 97–126. (In Chinese)
12. Chen, F.L.; Li, M.H.; Jiang, S.; Huang, C.; Zeng, D.D.; Chen, Y. An analysis of the climatological characteristics of precipitation in a heavy rain center of Northern Guangdong. *Guangdong Meteorol.* **2020**, *42*, 10–14. (In Chinese)
13. Chen, G.X.; Lan, R.Y.; Zeng, W.X.; Pan, H.; Li, W.B. Diurnal variations of rainfall in surface and satellite observations at the monsoon coast (South China). *J. Clim.* **2018**, *31*, 1703–1724. [CrossRef]
14. Du, Y.; Chen, G.X. Heavy rainfall associated with double low-level jets over Southern China. Part I: Ensemble-based analysis. *Mon. Wea. Rev.* **2018**, *146*, 3827–3844. [CrossRef]
15. Pu, Y.L.; Hu, S.; Luo, Y.L.; Liu, X.T.; Hu, L.H.; Ye, L.M.; Li, H.Q.; Xia, F.; Gao, L.Y. Multiscale perspectives on an extreme warm-sector rainfall event over coastal South China. *Remote Sens.* **2022**, *14*, 3110. [CrossRef]
16. Ye, L.M.; Liu, X.T.; Pu, Y.L.; Li, H.Q.; Xia, F.; Xu, B.Y. Contrasts in the evolution and microphysical features of two convective systems during a heavy rainfall event along the coast of South China. *Atmosphere* **2022**, *13*, 1549. [CrossRef]
17. Zhang, H.H.; Rao, X.N.; Guo, Z.Y.; Liu, X.T.; Yu, X.D.; Chen, X.D.; Li, H.Q.; Zhang, J.J.; Zeng, G.Y.; Chen, S.D. Detailed evolution characteristics of an inclined structure hailstorm observed by polarimetric radar over the South China coast. *Atmosphere* **2022**, *13*, 1564. [CrossRef]
18. Li, H.Q.; Huang, Y.J.; Hu, S.; Wu, N.G.; Liu, X.T.; Xiao, H. Roles of terrain, surface roughness, and cold pool outflows in an extreme rainfall event over the coastal region of South China. *J. Geophys. Res. Atmos.* **2021**, *126*, e2021JD035556. [CrossRef]
19. Feng, L.; Hu, S.; Liu, X.T.; Li, H.Q.; Xiao, H.; Li, X.H.; Lai, R.Z.; Lin, Q. Comparison of microphysical characteristics between warm-sector and frontal heavy rainfall in the South of China. *J. Trop. Meteorol.* **2023**, *29*, 87–100.
20. Liu, X.T.; Ruan, Z.; Hu, S.; Wan, Q.L.; Liu, L.P.; Luo, Y.L.; Hu, Z.Q.; Li, H.Q.; Xiao, H.; Lei, W.Y.; et al. The Longmen cloud physics field experiment base, China Meteorological Administration. *J. Trop. Meteorol.* **2023**, *29*, 1–15.
21. Si, D.; Xu, H.M.; Wen, M.; He, J.H. Analysis of the westward extension of western pacific subtropical high during a heavy rain period over southern china in June 2005. *J. Trop. Meteorol.* **2008**, *14*, 93–96.
22. Xiong, W.B.; Li, J.N.; Yao, C.; Wang, A.Y.; Fong, S.K. Analyzing continuous rainstorm in Southern China in June 2005. *J. Trop. Meteorol.* **2007**, *23*, 90–97. (In Chinese)
23. He, L.F.; Zhou, Q.L.; Chen, T. The evolution characteristics of mid-latitude and low-latitude synoptic systems during the "05·6" heavy rain event in South China. *J. Appl. Meteorol. Sci.* **2010**, *21*, 385–394. (In Chinese)
24. Wang, T.; Wu, C.S.; Fong, S.K. A Numerical Study of a Mesoscale Convective System Associated with the Heavy Rain Event over Guangdong Province in June 2005. *Chin. J. Atmos. Sci.* **2008**, *32*, 184–196. (In Chinese)
25. Xia, R.D.; Zhao, S.X. Diagnosis and modeling of meso-β-scale systems of heavy rainfall in warm sector ahead of front in South China (middle part of Guangdong Province) in June 2005. *Chin. J. Atmos. Sci.* **2009**, *33*, 468–488. (In Chinese)
26. Doswell, C.A., III; Brooks, H.E.; Maddox, R.A. Flash flood forecasting: An ingredients-based methodology. *Wea. Forecasting.* **1996**, *11*, 560–581. [CrossRef]
27. Sun, J.S.; Tao, Z.Y. Some essential issues connected with severe convective weather analysis and forecast. *Meteor Mon.* **2012**, *38*, 164–173. (In Chinese)

28. Yu, X.D. Nowcasting thinking and method of flash heavy rain. *Torrential Rain Disasters* **2013**, *32*, 202–209. (In Chinese)
29. Feng, L.; Lu, H.Q.; Li, F.; Liu, X.T.; Xiao, H.; Pan, X.; Xia, F. Characteristics of the raindrop size distribution in a squall line measured by two-dimensional video disdrometer in Guangdong. *J. Trop. Meteorol.* **2020**, *36*, 626–637. (In Chinese)
30. Sun, J.S.; Dai, J.H.; He, L.F.; Zheng, Y.Y.; Yu, X.D.; Xu, A.H. *Basic Principles and Technical Methods of Severe Convective Weather Forecast-Severe Convective Weather Forecast Manual of China*; Meteorological Press: Beijing, China, 2014; pp. 28–30. (In Chinese)